Journal of Thermal Analysis and Calorimetry, Vol. 90 (2007) 2, 385–392

STRUCTURAL AND THERMAL STUDIES ON THE SOLID PRODUCTS IN THE SYSTEM $MnSeO_3$–SeO_2–H_2O

L. T. Vlaev and Mariana P. Tavlieva*

Department of Physical Chemistry, Assen Zlatarov University, 8010 Bourgas, Bulgaria

The solubility of $MnSeO_3$–SeO_2–H_2O system was studied in the temperature region 25–300°C. The compounds of the three-component system were identified by the Schreinemaker's method. The phase diagram of manganese(II) selenites was drawn and the crystallization fields for the different phases were determined. Depending on the conditions for hydrothermal synthesis, $MnSeO_3 \cdot H_2O$, $MnSeO_3 \cdot 3/4H_2O$, $MnSeO_3 \cdot 1/3H_2O$ and $MnSe_2O_5$ were obtained. The different phases were proven and characterized by chemical, powder X-ray diffraction and thermal analyses, as well as IR spectroscopy. The kinetics of dehydration and decomposition of $MnSeO_3 \cdot H_2O$ was studied under non-isothermal heating. Based on 4 calculation procedures and 27 kinetic equations, the values of activation energy and pre-exponential factor in Arrhenius equation were calculated for both processes.

Keywords: *hydrothermal synthesis, IR spectroscopy, manganese(II) selenites, non-isothermal kinetic, powder X-ray diffraction, solubility diagrams, thermal analyses*

Introduction

Manganese(II) selenites are not found in nature as minerals [1]. Various manganese(II) selenites have been synthesized under different hydrothermal conditions [2–23]. Thus, $MnSeO_3 \cdot 2H_2O$ [4, 5, 11, 18], $MnSeO_3 \cdot H_2O$ [6, 10], $MnSeO_3 \cdot 3/4H_2O$ [19, 21], $MnSeO_3 \cdot 1/3H_2O$ [19, 21], $MnSeO_3$ [3, 4, 7, 9] and $MnSe_2O_5$ [8, 13, 14, 17] have been obtained. Manganese(II) hydrogen selenites have not been reported so far. The preparation and the thermal stability of $MnSeO_3 \cdot 2H_2O$ have been described in [4, 5, 11, 18]. The synthesis, the parameters of the crystal lattice, the spectroscopic and the magnetic behavior of $MnSeO_3 \cdot H_2O$ are given in [6, 15, 23]. The hydrothermal synthesis, the crystal structure, the spectroscopic and the magnetic properties of $MnSeO_3 \cdot 3/4H_2O$ and $MnSeO_3 \cdot 1/3H_2O$ are described in [19, 21]. The hydrothermal synthesis, the thermal, the spectroscopic and the magnetic properties of $MnSeO_3$ are described in [7, 9, 22]. The crystalline structure of $MnSe_2O_5$ and its vibration spectra are presented in [8, 13, 17], while its magnetic properties are described in [14]. The solubilities and the solubility products of various manganese(II) selenites are studied in [2, 16, 20]. Some of these selenites are used for coloring glasses, enamel and glazes. On the basis of $MnSeO_3$, two manganese selenides (α-MnSe and $MnSe_2$) were obtained having very interesting semiconductor properties [20].

The lack of systematic approach in most of the studies cited above does not allow to determine clearly the types and the number of the different solid phases which are in equilibrium with the liquid phase at various temperatures, as well as the boundaries of the crystallization fields of the known manganese(II) selenites in the system $MnSeO_3$–SeO_2–H_2O. In this respect, some useful information can be obtained from the dissolution isotherms of the system at different temperatures and the values of the parameters characterizing the non-variant (peritonic) points.

The aim of the present work is to study the crystallization fields of manganese(II) selenites in the system $MnSeO_3$–SeO_2–H_2O in the temperature interval 25–300°C and characterize the observed phases.

Experimental

Materials

The initial substance used was $MnSeO_3 \cdot H_2O$. It was prepared by precipitating 0.1 mol L^{-1} aqueous solution of manganese(II) dichloride tetrahydrate (puriss, Fluka) with 0.1 mol L^{-1} aqueous solution of sodium selenite pentahydrate, (puriss, Fluka) at 298 K at pH 7.2–8.0 [6]. The solutions with volumes of 1 L were slowly mixed (5 cm^3 min^{-1}) under continuous stirring with a blade mixer. The precipitate was left to 'age' in the initial solution at room temperature for a week. The formed crystalline substance was collected on a G4 frit, rinsed vigorously with distilled water and dried in air at ambient temperature for another week. The isolated compound was light-sepia coloured crystalline powder, which was stable in air at laboratory

* Author for correspondence: vlaev@btu.bg

1388–6150/$20.00

Akadémiai Kiadó, Budapest, Hungary
Springer, Dordrecht, The Netherlands

temperature. The results from the chemical and powder X-ray analyses showed it had net formula $MnSeO_3 \cdot H_2O$. Thus obtained, the $MnSeO_3 \cdot H_2O$ was used as initial substance for the study of the solubility in the $MnSeO_3$–SeO_2–H_2O system at different temperatures. Teflon-lined steel vessels (each having a volume of 20 cm^3) were used for the experiment [20]. 1 g $MnSeO_3 \cdot H_2O$ and 15 cm^3 aqueous solution of SeO_2 puriss (Merck) were placed in these vessels with concentrations varying from 0 to 70 mass% SeO_2 in 5% steps. The time required for equilibration of the individual samples was from 2 months (at 25°C) to 20 days (at 300°C). The temperatures of the hydrothermal synthesis are 25°C and from 50 to 300°C in 50°C steps. At the end of the experiment time, the vessels were cooled and opened and the precipitate was filtered through porous glass filter. Both the precipitate and the filtrate were analyzed to determine the contents of manganese(II) and selenium(IV). Selenium(IV) was determined iodometrically by Kotarski method [24]. Manganese(II) was titrated complexometrically using xylenol orange as an indicator [25]. The Schreinemaker's method was used to study the solubility in the $MnSeO_3$–SeO_2–H_2O system. The solubility diagram was drawn according to Gibbs–Roozeboom method [26].

Instrumental methods

Powder X-ray patterns were taken on a wide angle X-ray diffractometer goniometer URD-6, Freiberger Präzision Mechanik (Germany), using cells with a diameter of 12 mm, CuK_α radiation (λ=1.541870 Å) and an iron filter for β-emission. The lattice parameters were derived from 150–165 accurately measured reflections in the range $3 \le 2\theta \le 60°$. The structures were solved by Patterson method and refined with the least squares method.

The IR absorption spectra were taken on a spectrophotometer Specord-75 (Carl Zeiss, Jena, Germany) over the region from 400 to 4000 cm^{-1} (resolution 1 cm^{-1}). The experiments were carried out at room temperature using KBr pellets with concentration of the studied substance 0.3 mass%.

The thermal analyses of the samples were performed on a Paulik–Paulik–Erdey derivatograph (MOM, Hungary) by heating to 900°C at heating rate 6°C min^{-1} in a flow of nitrogen at a rate of 20 cm^3 min^{-1}. The samples (50 mg) were vigorously ground in an agate vibration mortar. The standard used was α-Al_2O_3 heated to 1100°C. The curves were registered with resolutions 1/5 for DTA, 1/15 for DTG and 1 mg for TG.

Kinetic parameters

The kinetics of the thermal dehydration and the decomposition of $MnSeO_3 \cdot H_2O$ at non-isothermal heating was studied by various equations [27], taking into account the special features of the process mechanism.

Several authors [28–31] suggested a few ways to calculate the kinetics parameters, characterizing the non-isothermal decompositions of the solids. For the present study, the calculation procedure of Coats and Redfern [28] was used. The data from TG and DTG curves in the decomposition range 0.1–0.9 were used to determine the kinetic parameters of the process according to these methods. The kinetic parameters can be derived using a modified Coats and Redfern (CR) equation:

$$\ln\frac{g(\alpha)}{T^2} = \ln\frac{AR}{qE} - \frac{E_A}{RT} \qquad (1)$$

where the expression of $g(\alpha)$ depends on the kinetic model of the occurring reaction [27]. If the correct $g(\alpha)$ is used, a plot of $\ln[g(\alpha)/T^2]$ *vs.* $1/T$ should give a straight line, from which the values of the activation energy E_A and the pre-exponential factor A in Arrhenius equation can be calculated. The formal expressions of the functions $g(\alpha)$ depend on the conversion mechanism and its mathematical model [27]. The latter usually represents the limiting stage of the reaction – the chemical reactions; random nucleation and nuclei growth; phase boundary reaction or diffusion. If the correct $g(\alpha)$ is used, the linear regression analysis of the corresponding linear dependence should give the highest correlation coefficient.

Later, some authors [29–31] suggested various equations, aiming to improve the accuracy of the kinetic parameters calculations. Thus, Madhusudanan–Krishnan–Ninan (MKN) [29] suggested the following equation:

$$\ln\left[\frac{g(\alpha)}{T^{1.921503}}\right] = \left[\ln\frac{AE_A}{qR} + 3.772050 - 1.921503\ln E_A\right] - 0.120394\frac{E_A}{T} \qquad (2)$$

Tang *et al.* (TL) [30] suggest another kinetic equation:

$$\ln\left[\frac{g(\alpha)}{T^{1.894661}}\right] = \left[\ln\frac{AE_A}{qR} + 3.63504095 - 1.894661\ln E_A\right] - 1.00145033\frac{E_A}{RT} \qquad (3)$$

and Wanjun *et al.* (WY) [31] proposed the equation:

$$\ln\left[\frac{g(\alpha)}{T^2}\right]= \ln\left[\frac{AR}{q(1.00198882E_A+1.87391198RT_p)}\right]-\frac{E_A}{RT} \quad (4)$$

Equations (1)–(4) imply that there are differences in the calculated values of the activation energy and pre-exponential factor A in Arrhenius equation, even with the same $g(\alpha)$ function. The value of the coefficient of correlation in the linear regression R^2 for Eqs (1)–(4) was used as criterion for the estimation of the four calculating procedures aiming to find the most suitable one. For the calculations of the kinetic parameters, a computer program was developed for all the data manipulations.

The values of the pre-exponential factor A in Arrhenius equation for solid phase reactions are expected to be quite wide ranged (six or seven orders of magnitude), even after the correction of the surface area effect [32, 33]. The empirical first order pre-exponential factors may vary from 10^5 to 10^{18} s^{-1}. The low factors will often indicate a surface reaction, but if the reactions are not dependent on the surface area, the low factor may indicate a 'tight' complex. The high factors will usually indicate a 'loose' complex. Even higher factors (after correction of the surface area) can be obtained if the complexes have free translation on the surface. Since the concentrations in solids are not controllable in many cases, it would be convenient if the magnitude of the pre-exponential gives an indication of the reaction molecularity. This appears to be true only for non-surface-controlled actions having low (<10^9 s^{-1}) pre-exponential factors. According to the theory of the activated complex (transition state) of Eyring [32, 33]:

$$A=\frac{e\chi k_B T_p}{h}\exp\left(\frac{\Delta S^{\#}}{R}\right) \quad (5)$$

where e=2.7183 is the Neper number; χ – transition factor, which is unity for monomolecular reactions; k_B – Boltzmann constant; h – Plank constant, and T_p is the peak temperature of DTA curve. Using Eq. (5), the change of entropy for the formation of the activated complex of the reagent can be calculated:

$$\Delta S^{\#}=R\left(\ln\frac{Ah}{e\chi k_B T_p}\right) \quad (6)$$

Since

$$\Delta H^{\#}=E_A-RT_p \quad (7)$$

the changes of the enthalpy $\Delta H^{\#}$ and Gibbs free energy $\Delta G^{\#}$ for the activated complex formation from the reagent can be calculated using the well known thermodynamical equation:

$$\Delta G^{\#}=\Delta H^{\#}-T_p\Delta S^{\#} \quad (8)$$

The values of $\Delta S^{\#}$, $\Delta H^{\#}$ and $\Delta G^{\#}$ were calculated at $T=T_p$, since this temperature characterizes the highest rate of the process and, therefore, is its important parameter.

Results and discussion

The Schreinemakers' method [26] was used to study solubility in the $MnSeO_3$–SeO_2–H_2O system at different temperatures. Despite that the system was studied at 25, 50, 100, 150, 200, 250 and 300°C, only the solubility diagrams obtained at 25, 150 and 250°C are presented

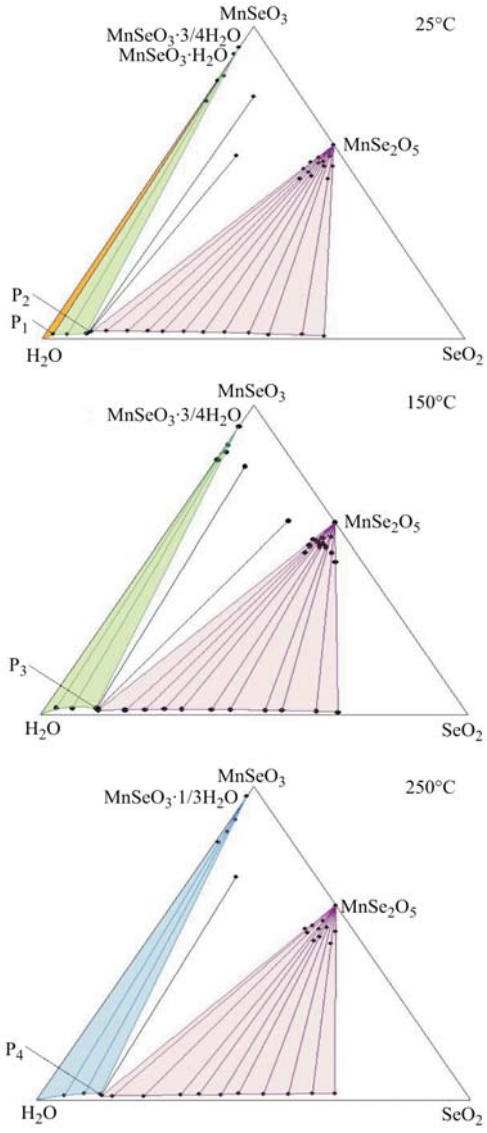

Fig. 1 Solubility isotherms of the system $MnSeO_3$–SeO_2–H_2O at different temperatures

on Fig. 1, constructed by the Gibbs–Roozeboom method.

Schreinemakers' data showed that three solid phases crystallize in the system at 25°C – $MnSeO_3·H_2O$, $MnSeO_3·3/4H_2O$ and $MnSe_2O_5$. The first peritonic point (P_1) between $MnSeO_3·H_2O$ and $MnSeO_3·3/4H_2O$ is at 1.61 mass% $MnSeO_3$, 0.80 mass% SeO_2 and 97.60 mass% H_2O. The second peritonic point (P_2) between $MnSeO_3·3/4H_2O$ and $MnSe_2O_5$ is at 1.88 mass% $MnSeO_3$, 3.38 mass% SeO_2 and 94.74 mass% H_2O.

At 150°C, Schreinemakers' data showed that only two solid phases crystallize in the system – $MnSeO_3·3/4H_2O$ and $MnSe_2O_5$. The peritonic point P_3 corresponds to 2.45 mass% $MnSeO_3$, 4.43 mass% SeO_2 and 93.13 mass% H_2O.

At 250°C, two solid phases crystallize in the system as well – $MnSeO_3·1/3H_2O$ and $MnSe_2O_5$. The peritonic point P_4 corresponds to 1.75 mass% $MnSeO_3$, 10.48 mass% SeO_2 and 87.78 mass% H_2O.

The results from the experiments showed that the following solid phases had been formed in the system $MnSeO_3$–SeO_2–H_2O which was in equilibrium with the liquid phase (containing from 0 to 70 mass% SeO_2) within the temperature interval 25–300°C: $MnSeO_3·H_2O$ ($MnO·SeO_2·H_2O$), $MnSeO_3·3/4H_2O$ ($MnO·SeO_2·3/4H_2O$), $MnSeO_3·1/3H_2O$ ($MnO·SeO_2·1/3H_2O$) and $MnSe_2O_5$ ($MnO·2SeO_2$). The polythermal diagram of the studied system was drawn on the basis of the solubility isotherms of $MnSeO_3$–SeO_2–H_2O system at different temperatures and the compositions at the peritonic points in the Gibbs–Rooseboom diagrams (Fig. 2).

As can be seen from the figure, four different crystallization fields can be identified as well as one none variant point with three solid phases ($MnSeO_3·3/4H_2O$, $MnSeO_3·1/3H_2O$ and $MnSe_2O_5$) in equilibrium. The smallest field area corresponded to the phase $MnSeO_3·H_2O$ existing at temperatures below 100°C and SeO_2 concentrations lower than 2.5 mass%. With the increase of the temperature to 185°C and SeO_2 concentration to 10.0 mass%, a crystallization field was formed for $MnSeO_3·3/4H_2O$. The field of the solid phase of $MnSeO_3·1/3H_2O$ formed at temperatures above 185°C. The largest crystallization field area was that for $MnSe_2O_5$, which formed at SeO_2 concentrations higher than 10 mass% and temperatures from 25 to 300°C. If the composition of the different selenites is described by the general formula $MnO·nSeO_2·mH_2O$, then Fig. 2 shows that phases with small m have become stable with the increase of the temperature while the phases with small n have been more stable at lower SeO_2 concentration. At SeO_2 concentration lower than 10 mass%, the increase of temperature have led to formation of thermodynamically stable selenite phases with lower values of m: $MnSeO_3·H_2O \rightarrow MnSeO_3·3/4H_2O \rightarrow MnSeO_3·1/3H_2O$. The results clearly show that the hydrothermal treatment of $MnSeO_3·H_2O$ does not give $MnSeO_3$ in the studied temperature and concentration intervals. According to some authors [5, 6], the reason of this lack of continuity was the incompatibility of the texture of these crystal phases.

All individual phases of the manganese(II) selenites were of the same colour (light-sepia) and crystalline habitus. The samples were identified by the chemical, X-ray diffraction and IR spectroscopy

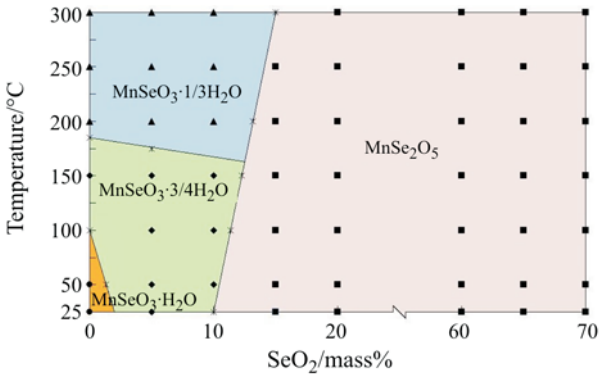

Fig. 2 Crystallization field of selenites in the system $MnSeO_3$–SeO_2–H_2O

Table 1 Crystallographic data for different manganese(II) selenites

Parameter	$MnSeO_3·H_2O$ [23]	$MnSeO_3·3/4H_2O$ [21]	$MnSeO_3·1/3H_2O$ [19, 21]	$MnSe_2O_5$ [8, 14]
Space	$P2_1/n$	$P2_1$	P-1	Pbcn
group	4.921(3)	9.181(2)	8.266(3)	6.797(2)
a/Å	13.121(7)	8.602(3)	8.350(3)	10.617(3)
b/Å	5.816(1)	9.852(4)	9.008(3)	6.300(2)
c/Å	–	–	65.24(3)	–
α/°	90.03(2)	116.63(2)	68.82(4)	–
β/°	–	–	67.77(4)	–
γ/°	4	2	2	4
V/Å^3	375.5(4)	695.5(4)	507.2(3)	454.6
d_R/g cm^{-3}	3.499	3.6(1)	3.6(1)	4.21

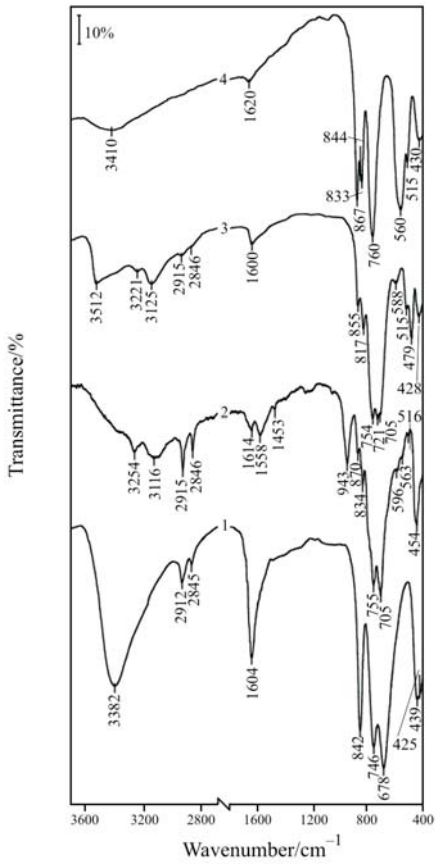

Fig. 3 Infrared absorption spectra of manganese(II) selenites at 25°C: 1 – $MnSeO_3 \cdot H_2O$, 2 – $MnSeO_3 \cdot 3/4H_2O$, 3 – $MnSeO_3 \cdot 1/3H_2O$ and 4 – $MnSe_2O_5$

analyses. On the basis of the recorded X-ray diffractograms the parameters of the crystalline unit cells were calculated for the synthesized selenites. They were found to be almost the same as those reported by other authors [8, 14, 15, 19, 21]. The parameters characterizing the crystalline lattices of the selenites are summarized in Table 1.

The different manganese(II) selenites were studied by IR spectroscopy and the absorption spectra are presented in Fig. 3.

The bands have been interpreted according to the works of some authors [6, 19, 21, 34–37] who have been studying IR spectra of different selenites. Figure 3 shows that IR spectra of the studied selenites have some common and some specific bands. In the high frequency region of IR spectra (2800–3500 cm^{-1}), for instance, some absorption bands were registered which should be attributed to stretching vibrations of O–H from H_2O molecules. In the middle frequency region (1400–1620 cm^{-1}), absorption bands with different intensities were observed and attributed to the bending vibrations of H_2O molecules. The different vibration frequencies for the crystallohydrates were considered to be due to the different locations and strengths of water molecule bonds in the selenites crystalline lattice. It should be noted that the bands intensity decreased with the decrease of the amount of crystallization water but the number of absorption bands increased. It was due to the weakening of the masking effect of the bigger amounts of water and revealing of the superfine structure of the crystallohydrates. A number of bands were registered in the low frequency region (400–900 cm^{-1}) and their number increased from $MnSeO_3 \cdot H_2O$ to $MnSe_2O_5$, i.e. as dehydration proceeded, the characteristic bands were more distinctly measured and the IR spectrum had more details. Three types of characteristic bands were found: $\nu_{(Se–O)}$ in SeO_3^{2-} anion, $\nu_{(Mn–O)}$ and $\delta_{(O–Se–O)}$. These absorption bands were observed in the IR spectra of the other selenites; they were carefully analysed by other authors [19, 21, 34–37].

The spectrum of $MnSe_2O_5$ (Fig. 3, spectrum 4) showed two low intensity and wide absorption bands at 3410 and 1620 cm^{-1}. They were due to the stretching and bending vibrations of small amounts of water physically adsorbed on the sample surface. Taking into account the composition and the specific features of the diselenites thermal decomposition, $MnSe_2O_5$ can be regarded as a product of attachment – co-ordination bonding of a molecule SeO_2 to $MnSeO_3$. Therefore, the IR spectrum showed both absorption bands for the almost free SeO_2 [19, 21] and ions [34–37]. The large number of bands present in the interval 870–400 cm^{-1} is usually connected with the vibration structure of the diselenite anion [$O_2Se–O–SeO_2$]. The spectrum is considered to summarize the vibrations of (SeO_2)-groups and (Se–O–Se) bridges [34–37]. According to the authors who have studied various selenites, the bands observed in the interval 950–860 cm^{-1} are due to $\nu_{as(SeO_2)}$; 840–810 cm^{-1} – to $\nu_{s(SeO_2)}$; 760–740 cm^{-1} – $\nu_{s(Se–O–Se)}$; 720–670 cm^{-1} – $\nu_{as(Se–O–Se)}$; 480–380 cm^{-1} – $\delta_{(SeO_2)}$ and those from 300 to 250 cm^{-1} – to $\delta_{(Se–O–Se)}$. The weak band at 515 cm^{-1} belongs to $\nu_{(Mn–O)}$. All the registered IR absorption bands of the studied selenites are summarized in Table 2 together with their assignments.

The TG, DTG and DTA curves of thermal dehydration and decomposition of manganese(II) selenite monohydrate are presented on Fig. 4.

The DTA shows endothermal peak at 553 K corresponding to one step dehydration of the monohydrate and the final mass loss (9.0%) indicates for practically stoichiometric dehydration. In accordance with the data, presented in [6], the dehydration process of $MnSeO_3 \cdot H_2O$, $CoSeO_3 \cdot H_2O$, $NiSeO_3 \cdot H_2O$ and $ZnSeO_3 \cdot H_2O$ pass in a single step in narrow temperature interval at 570, 620, 730 and 500 K, respectively. Larranaga *et al.* [21] reported that two new manganese(II) selenites with the formula $MnSeO_3 \cdot 3/4H_2O$ and $MnSeO_3 \cdot 1/3H_2O$ have been synthesized only by using mild hydrothermal

Table 2 Infrared absorption spectra of different manganese(II) selenites: ν/cm^{-1}

$MnSeO_3 \cdot H_2O$	$MnSeO_3 \cdot 3/4H_2O$	$MnSeO_3 \cdot 1/3H_2O$	$MnSe_2O_5$	Band assignment
	425 sh	428 m	430 m	$\delta_{(SeO_2)}$
425 sh	454 s	479 s		$\delta_{(SeO_2)}$
439 vs	516 w	515 w	515 w	$\nu_{(Mn-O)}$
			560 vs	$\nu_{as(Se-O-Se)}$
	705 vs	721 vs		$\nu_{as(Se-O)(SeO_3^{2-})}$
678 vs	755 vs	754 vs	760 vs	$\nu_{s(Se-O)(SeO_3^{2-})}$
746 vs	834 w	817 w	833 s	$\nu_{s(SeO_2)}$
842 vs	870 w	855 w	867 vs	$\nu_{as(SeO_2)}$
	943 s			$\nu_{as(SeO_2)}$
	1558 m			$\delta_{(HOH)(H_2O)}$
1064 vs	1614 w	1600 m	1620 m	$\delta_{(HOH)(H_2O)}$
2845 w	2846 m	2846 w		$\nu_{(O-H)(H_2O)}$
2912 w	2915 s	2915 w		$\nu_{(O-H)(H_2O)}$
	3116 b	3125 m		$\nu_{(O-H)(H_2O)}$
3382 vs	3254 w	3512 s	3410 b	$\nu_{(O-H)(H_2O)}$

vs – very strong, s – strong, m – medium, w – weak, b – broad, sh – shoulder, ν – stretching, ν_s – symmetric stretching, ν_{as} – antisymmetric stretching and δ – bending vibration

conditions under autogeneous pressure. No data have been obtained for low crystallohydrates as stable intermediate forms by using thermal dehydration of manganese(II) selenite monohydrate. The dehydration of $MnSeO_3 \cdot 2H_2O$ and $ZnSeO_3 \cdot 2H_2O$ pass in two steps [11]. According to Verma and Khushu [35], the reason for this lies in the fact that the two water molecules are not in equivalent positions; hence they are not energetically equal. The anhydrous manganese(II) selenite completely dissociated (endothermal peak at 843 K and mass loss 55.5%) to MnO and SeO_2 without melting. The data for the TG curve were processed according to the four calculation procedures and the kinetic equations shown in [27], aiming to obtain a maximum value of the correlation coefficient R^2. Regardless of the calculation procedure, the highest value of R^2 was found when the function $g(\alpha)=[(1-\alpha)^{-1/2}-1]$ corresponding to a kinetic equation with n=1.5 was used. The values of the correlation coefficient obtained with the four procedures were quite close which did not give enough grounds to select one of them. For illustration, the dependence $\ln\lfloor g(\alpha)/T^{1.894661}\rfloor = f(1/T)$ calculated by the procedure of Tang *et al.* [30] with $g(\alpha)=[(1-\alpha)^{-1/2}-1]$ which happened to produce the maximal values of R^2, is presented in Fig. 5.

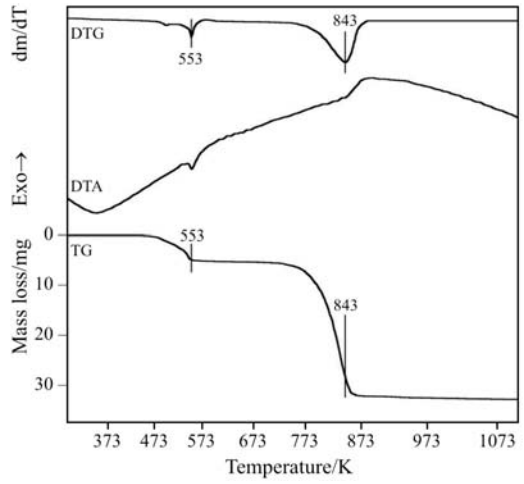

Fig. 4 TG, DTG and DTA curves of dehydration and decomposition of $MnSeO_3 \cdot H_2O$

Based on the linear dependences shown in Fig. 5 and using Eq. (3), the values of the activation energy E_A and pre-exponential factor A in the Arrhenius equation for $MnSeO_3 \cdot H_2O$ dehydration and decomposition were calculated and the corresponding values of $\Delta S^{\#}$, $\Delta H^{\#}$ and $\Delta G^{\#}$ were obtained using Eqs (6)–(8). The values of these parameters, which have been obtained according to the calculation procedures of Coats–Redfern [28], Madhusudanan–Krishnan–Ninan [29], Tang *et al.* [30] and Wanjun *et al.* [31] are presented in Table 3.

As can be seen from Table 3, the values of the activation energy E_A and the pre-exponential factor A in Arrhenius equation are practically equal regardless

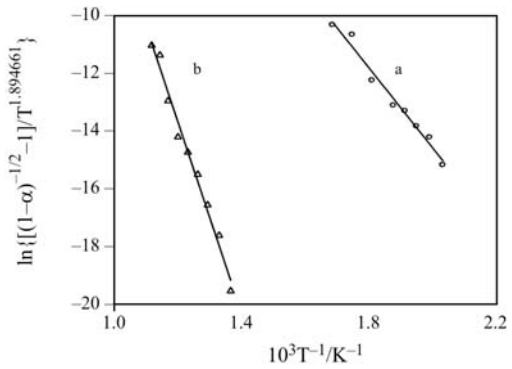

Fig. 5 Dependence of $\ln\lfloor g(\alpha)/T^{1.894661}\rfloor$ [30] *vs.* $(1/T)$ for: a – dehydration and b – decomposition of $MnSeO_3 \cdot H_2O$

Table 3 Kinetic parameters of non-isothermal dehydration and decomposition of $MnSeO_3 \cdot H_2O$

Parameter	Calculation procedure			
	CR	MKN	TL	WY
		Dehydration of $MnSeO_3 \cdot H_2O$		
Symbol	$F_{3/2}$	$F_{3/2}$	$F_{3/2}$	$F_{3/2}$
R^2	0.9880	0.9881	0.9883	0.9880
E_A/kJ mol^{-1}	116.1	116.3	116.4	116.1
A/min^{-1}	$2.63 \cdot 10^{10}$	$2.97 \cdot 10^{10}$	$3.03 \cdot 10^{10}$	$2.83 \cdot 10^{10}$
$\Delta S^{\#}$/J K^{-1}mol^{-1}	–92.9	–91.9	–91.7	–92.3
$\Delta H^{\#}$/kJ^{-1}mol^{-1}	111.5	111.7	111.8	111.5
$\Delta G^{\#}$/kJ^{-1}mol^{-1}	162.9	162.6	162.5	162.5
T_p/K		553		
		Decomposition of $MnSeO_3$		
Symbol	$F_{3/2}$	$F_{3/2}$	$F_{3/2}$	$F_{3/2}$
R^2	0.9942	0.9943	0.9944	0.9942
E_A/kJ mol^{-1}	277.3	277.6	277.6	277.3
A/min^{-1}	$2.87 \cdot 10^{16}$	$3.12 \cdot 10^{16}$	$3.14 \cdot 10^{16}$	$3.01 \cdot 10^{16}$
$\Delta S^{\#}$/J K^{-1}mol^{-1}	19.2	19.9	19.9	19.6
$\Delta H^{\#}$/kJ^{-1}mol^{-1}	270.3	270.5	270.6	270.3
$\Delta G^{\#}$/kJ^{-1}mol^{-1}	254.1	253.8	253.8	253.8
T_p/K		843		

The values of $\Delta S^{\#}$, $\Delta H^{\#}$ and $\Delta G^{\#}$ were calculated at the corresponding peak temperature T_P

of the calculation procedure used. The dehydration of $MnSeO_3 \cdot H_2O$, however, is characterized by significantly lower values of E_A and A compared to the decomposition of $MnSeO_3$. Similar tendency is observed in the kinetics of dehydration and decomposition of $CoSeO_3 \cdot 2H_2O$ and $NiSeO_3 \cdot 2H_2O$ [38, 39]. The big difference between the values of the pre-exponential factor A for the processes of dehydration and decomposition of selenites is interesting. According to some authors [40], values of A about $1.0 \cdot 10^{16}$ have been regarded as a proof that the complex has a 'free' condition unlike the reactants. This may most likely occur on a surface where the complex extends itself from the surface and perhaps rotates parallel to the surface. In this case the reactant is assumed to be completely restricted. In the cases when the values of A are about $1.0 \cdot 10^{10}$, the complex has been considered to be highly restricted in rotation [40]. For the unimolecular case, the complex is expected to expand in size and hence interact more intensely with its neighbours. The formation of the activated complex of the reagent reflects in a specific way on the change of the entropy $\Delta S^{\#}$. Thus, $\Delta S^{\#}$ is negative for the dehydration of the selenites but positive for its decomposition. The negative value of $\Delta S^{\#}$ means that the activated complex of the reagent has higher degree of arrangement than the initial reagent while the negative value indicates the opposite. Therefore, the effects of the entropy factor on the rates of dehydration and decomposition are contrary.

Conclusions

It may be concluded that the absorption bands observed in the IR spectra of the different selenites studied, together with the results from the powder X-ray diffraction and chemical analyses, irrefutably prove the existence of different crystalline forms of manganese(II) selenites and provide enough data to determine the corresponding crystallization fields of stability in the solubility diagram of the system $MnSeO_3$–SeO_2–H_2O. The values of the activation energy found for the dehydration and decomposition processes of the manganese(II) selenites studied showed, that the dehydration occurs with relatively low value of the activation energy and negative change of entropy while the decomposition requires higher activation energy and is accompanied by positive change of entropy for the formation of the activated complex of the reagent.

References

1 J. A. Mandarino, Eur. J. Mineral., 6 (1994) 337.
2 V. G. Chukhlantzev and G. P. Tomashevskii, Zh. Anal. Khim., 12 (1957) 296.
3 E. A. Buketov, Vest. An KazSSR, Ser. Khim., 21 (1965) 30.
4 Z. L. Lestinskaya and N. M. Selivanova, Izv. VUZ, Khim. Khim. Tekhnol., 4 (1966) 523.
5 O. J. Lieder and G. Gattow, Naturwissenschaften, 54 (1967) 443.
6 V. N. Makatun, R. Ya. Melnikova and T. I. Barannikova, Koord. Khim., 1 (1975) 920.

7 K. Kohn, S. I. Akimoto, K. Inoue, K. Asai and O. Horie, J. Phys. Soc. Jpn., 38 (1975) 587.
8 M. Koskenlinna, L. Ninisto and J. Valkonen, Acta Chem. Scand. A, 30 (1976) 836.
9 K. Kohn, K. Inoue, O. Horie and S. I. Akimoto, J. Solid State Chem., 18 (1976) 27.
10 M. Koskenlinna and J. Valkonen, Acta Chem. Scand. A, 31 (1977) 752.
11 R. Ya. Melnikova, V. N. Makatun, V. V. Pechkovskii, A. K. Potapovich and V. Z. Drapkia, Zh. Neorg. Khim., 23 (1978) 691.
12 B. L. Khandelwal and S. P. Mallela, Thermochim. Acta, 33 (1979) 355.
13 G. Giester and M. Wildner, J. Solid State Chem., 91 (1991) 370.
14 J. Bonvoisin, J. Galy and J.-C. Trombe, J. Solid State Chem., 107 (1993) 171.
15 B. Engelen, U. Baumer, B. Hermann, H. Miller and K. Unterderweide, Z. Anorg. Allg. Chem., 622 (1996) 1886.
16 S. Sharamasarkar, K. J. Reddy and G. F. Vance, Chem. Geol., 132 (1996) 165.
17 A. B. Gopinath and S. Devanarayanan, Int. J. Modern Phys. B, 13 (1999) 2645.
18 V. P. Verma, Thermochim. Acta, 327 (1999) 63.
19 A. Larranaga, J. L. Pizarro, J. L. Mesa, M. I. Arriortua and T. Rajo, Bol. Soc. Esp. Miner., 24-A (2001) 17.
20 Q. Peng, Y. Dong, Z. Deng, H. Kou, S. Gao and Y. Li, J. Phys. Chem. B, 106 (2002) 9261.
21 A. Larranaga, J. L. Mesa, J. L. Pizarro, R. Olazcuaga, M. I. Arriortua and T. Rajo, J. Chem. Soc., Dalton Trans, 18 (2002) 3447.
22 A. Larranaga, J. L. Mesa, J. L. Pizarro, L. Lezama, J. P. Chapman, M. I. Arriortua and T. Rajo, J. Chem. Soc., Dalton Trans., 21 (2005) 1727.
23 A. Larranaga, J. L. Mesa, J. L. Pizarro, A. Pena, R. Olazcuaga, M. I. Arriortua and T. Rajo, J. Solid State Chem., 178 (2005) 3686.
24 A. Kotarski, Chem. Anal., 10 (1965) 161.
25 R. Pribil, Complexonometry (in Bulgarian), Thehnika, Sofia 1980.
26 M. H. Karapetyanz, Chemical Thermodynamics (in Russian), Moscow, Khimiya 1975, pp. 315–318.
27 L. T. Vlaev, V. G. Georgieva and S. D. Genieva, J. Therm. Anal. Cal., OnlineFirst: DOI: 10.1007/s10973-005-7149-y.
28 A. W. Coats and J. P. Redfern, Nature (London), 201 (1964) 68.
29 P. M. Madhusudanan, K. Krishnan and K. N. Ninan, Thermochim. Acta, 221 (1993) 13.
30 W. Tang, Y. Liu, H., Zhang and C. Wang, Thermochim. Acta, 408 (2003) 39.
31 T. Wanjun, L. Yuwen, Z. Hen, W. Zhiyong and W. Cunxin, J. Therm. Anal. Cal., 74 (2003) 309.
32 J. Šesták, Thermodynamical properties of solids, Academia Prague, 1984.
33 J. M. Criado, L. A. Pérez-Maqueda and P. E. Sánchez-Jiménez, J. Therm. Anal. Cal., 82 (2005) 671.
34 G. G. Gospodinov, L. M. Sukova and K. I. Petrov, Zh. Neorg. Khim., 33 (1988) 1970.
35 V. P. Verma and A. Khushu, J. Thermal Anal., 35 (1989) 1157.
36 M. Ebert, Z. Micka and I. Pekova, Chem. Zvesti, 36 (1982) 169.
37 M. Ebert, Z, Micka and I. Pekova, Coll. Czech. Chem. Comm., 47 (1982) 2069.
38 L. T. Vlaev, S. D. Genieva and G. G. Gospodinov, J. Therm. Anal. Cal., 81 (2005) 469.
39 L. T. Vlaev, S. D. Genieva and V. G. Georgieva, J. Therm. Anal. Cal., 86 (2006) 449.
40 H. F. Cordes, J. Phys. Chem., 72 (1968) 2185.

Received: February 15, 2007
Accepted: March 20, 2007
OnlineFirst: June 1, 2007

DOI: 10.1007/s10973-007-7748-x